Is the Western Himalayan region vulnerable in respect to downscaled precipitation?

Jitendra Kumar Meher
Bidhan Chandra Krishi Viswavidyalaya (BCKV)
Lalu Das (daslalu@yahoo.co.in)
Bidhan Chandra Krishi Viswavidyalaya (BCKV)

Research Article

Keywords: Statistical Downscaling, Western Himalaya Region, Precipitation, Monsoon, Global Climate Model

Posted Date: February 17th, 2022

DOI: https://doi.org/10.21203/rs.3.rs-1358116/v1

Version of Record: A version of this preprint was published at Theoretical and Applied Climatology on April 12th, 2022. See the published version at https://doi.org/10.1007/s00704-022-04048-x.

Is the Western Himalayan region vulnerable in respect to downscaled precipitation?

Jitendra Kumar Meher and Lalu Das*

Department of Agricultural Meteorology and Physics,

Bidhan Chandra Krishi Viswavidyalaya (BCKV),

West Bengal, India. 741252

*Corresponding Author:

Prof (Dr) L. Das

Email: daslalu@yahoo.co.in

ABSTRACT

Statistical downscaling is the technique of linking large-scale predictors and local scale predictand through a relationship that is assumed to be useful to generate local scale climate change information from GCMs driven large-scale future projection. An attempt has been made to construct downscaled seasonal and annual rainfall change scenarios over different station locations of the Western Himalaya Region (WHR) of India using common predictors from ten Global Climate Model (GCM) of CMIP5 (Coupled Model intercomparison Project phase 5) and reanalysis datasets from NCEP/NCAR datasets (National Centers for Environmental Prediction/ National Center for Atmospheric Research); and predictands from the IMD (India Meteorological Department) rain gauge stations. Combined EOF (Empirical Orthogonal Function) approach has been used to develop stations specific statistical downscaling models over the WHR and later on some statistical skill scores based on error and agreement analysis were used to validate the model performance. Downscaled precipitation scenario using multi model ensemble of GCM under RCP4.5 (Representative concentration pathways 4.5) revealed a wetter climate during the 2020s, 2050s and 2080s in the annual and monsoon time scale, whereas a drier climate is expected in the winter season. Results reveal a possible intensification of south-west monsoon and decrease in the frequency of western disturbances in the 21st century as the percentage changes of rainfall in monsoon were higher compared to annual and winter timescale. The uncertainty in the monthly precipitation is predicted to increase as the time progresses during 2020s to 2080s. Higher uncertainty in precipitation is expected in the late pre-monsoon months and early post-monsoon month over the study region.

Key Words: Statistical Downscaling; Western Himalaya Region; Precipitation; Monsoon; Global Climate Model

1. Introduction

Under the context of global warming, the uneven gradual increment in surface air temperature in different parts of the globe may lead to change in precipitation patterns and intensity adversely on local scale, resulting the serious threat to our day-to-day agricultural activities and hydrological systems. The impact is more serious over the areas covered with snow and ice like the Himalayan region. So accurate assessment of precipitation change over sub-regional and local scale of a topographic region is more important than the assessment of GCMs driven mean precipitation (Benestad et al. 2007; Das et al 2016). Change of precipitation over mountainous regions significantly impacts the life and livelihood million of people living therein and neighbouring plain areas as the melt and surface rainwater can serve the lifelines of all rivers and streams. As per the fifth assessment report of the Intergovernmental Panel on Climate Change (IPCC: AR-5, 2013), the Himalayas are considered to be a hot spot of climate change. They are a spectacular range of mountains located in the subtropical high-pressure belt region of the planet earth and encompasses parts of eight South Asian territories of Afghanistan, Pakistan, China, India, Nepal, Bhutan, Bangladesh, and Myanmar. The glaciers present in the Himalayas feed water to the numerous rivers flowing across the Indo-Gangetic plains. The weather in the Himalayas is quite unpredictable due to unexpected occurrences of snowstorms, high winds, cloudbursts etc, resulting in sudden floods (Nandargi and Dhar 2011). Due to the vagaries of local precipitation, several devastating floods have left their footprints over the Western Himalayan region (WHR) during the recent past - Leh-Ladakh floods of 2010 , Western Himalayan floods of 2012, Uttarakhand floods of 2013, Jammu and Kashmir flood of 2014 etc. (Ghawana and Minoru 2015; Sati and Gahalaut 2013). These floods not only wiped out thousands of lives but also damaged property and destructed crops. So, the basic question arises in mind is, what will be the future scenario under such natural disasters? One of the possible answers lies in the analysis of the ‘projections of future rainfall events’.

It is important to infer local precipitation through the means of so-called 'downscaling' in GCM studies. Downscaling is the process in which a real and physical linkage is developed between the state of some variable representing a large space/scale (e.g. Sea level pressure) and the state of some variable representing a smaller space/scale (e.g. Local temperature of a weather

station) (Benestad et al. 2008; Benestad 2011; Chen et al. 2014). The large-scale variables are often termed as predictors or independent variables, and the smaller scale variables are called as predictand or dependent variable.

One of the major limitations of the use of Global Climate Models (GCM) is the raw outputs derived from GCMs are practically of no use over a smaller region (Wilby et al. 1999; Benestad et al. 2008; Meher et al. 2014) because of their inherent biases and uncertainty to reproduce local scale features. GCMs may contain systematic biases or errors; in addition, the processes described inside GCMs are based on parameterization and may not be stationary (Meher et al. 2017). Hence the necessity of downscaling technique aroused to bridge this gap (Benestad et al 2007; Benestad et al. 2008; Meher et al. 2017). The results from the GCMs can be downscaled in two different ways; (i) downscaling through a nested high-resolution Regional Climate Model (RCM) often termed as 'Dynamical downscaling' illustrating the atmospheric and surface state in a smaller area with an enhanced spatial resolution than the GCM and (ii) Statistical downscaling or Empirical-Statistical Downscaling (ESD) (Wilby and Wigley 1997; Timbal et al. 2008; Benestad et al. 2008; Benestad 2011; Chen et al. 2014). Some properties of GCMs are also common to the RCMs like the bias and parameterization. One of the major difficulties in assessing RCMs is they require large computer resources, while GCMs can be assessed through ordinary computers (Benestad 2008).

The purpose of ESD is very specific, such as using GCMs to make an assumption about the local climate at a given location. Application of ESD to scenarios from GCMs was recommended by intergovernmental panel on climate change (IPCC) to produce local description with fine scale structures (IPCC, 1995). ESD involves statistically representing appropriate fields from coarser resolution GCMs. This method is more economical and less computer intensive, because, it doesn't involve complex atmospheric physics (Benestad 2011; Blazak 2012; Salvi et al., 2013; Sachindra et al., 2014). However, ESD requires a large volume of authentic data to begin with, a suitable set of predictors and the notion that the relationship between these predictors and the predictand will remain valid in the future climate (Benestad 2011; Blazak 2012). This approach is known as perfect prognosis (PP) (Maraun et al., 2010; Chen et al. 2014). There are three types of statistical downscaling schemes – (i) Transfer function (based on

regression models), (ii) Weather typing/weather classification schemes, and (iii) weather generators (Wilby et al., 2004, Benestad 2008; Blazak 2012; Chen et al. 2014). First two types of scheme may involve a pp-approach (Kanan et al. 2013) which use empirical models that relate observation-based predictand and large-scale predictor during a common time period and then applied to simulated predictors (for example GCM scenario runs) for the future (Kanan et al. 2013; Eden & Widmann 2014). In addition, a common attribute for many of these schemes is to apply an empirical orthogonal function (EOF) analysis to the large-scale variables (predictor) using few leading EOFs to train the empirical models (Zorita and von Storch 1999; Benestad 2001b; Benestad et al. 2008; Benestad 2010; Das et al. 2016). To be very specific, the 'first scheme' deals with the linking of local scale climate variables with large-scale atmospheric field by the use of a linear or non-linear regression model (Blazak 2012; Chen et al. 2014; Das et al. 2016). Under this scheme, a statistical equation is developed that can incorporate one or more large-scale predictor variables to estimate the local scale predictand. The 'second scheme' group days into similar synoptic events and relates those with local conditions such as temperature and precipitation (Blazak 2012). The third scheme uses stochastic models based on a gamma distribution for rainfall amounts and a Markov chain or semi-empirical distribution for transition probabilities between states. Under this scheme, a long series of daily and sub-daily weather data can be produced which has been able to capture the extreme events (Semenov and Barrow 2002; Semenov 2008; Blazak 2012). The present study deals with the first scheme of downscaling i.e. the transfer function.

The transfer function based statistical downscaling is most popular and widely used technique to project rainfall and temperature for future. The quality and the reliability of results obtained from ESD for successful implication in the local scale depends on various factors like long-term data with fewer missing records, local scale variable (predictand) to be downscaled, geography and circulation pattern of the site under consideration, and most importantly selection of a suitable predictor/s. Predictand like temperature shows >70% variance in most of the downscale result, while for rainfall the variance reduces to ~30% (Wilby et al., 1999; Chen et al. 2014). To overcome this issue, bias correction of downscaled results can be carried out as done in the statistical downscaling model (SDSM) (Wilby et al. 2002b). The most frequently used

predictors from GCM outputs for downscaling precipitation over the Indian and surrounding region include Geopotential height, mean sea level pressure, air temperature, perceptible water content, precipitation rate, zonal and meridional velocity, relative humidity, and specific humidity (Huth et al. 1999; Goyal and Ojha 2010; Ojha et al. 2010; Huang et al. 2011; Blazak 2012; Mahmood and Babel 2012; Hu et al. 2013; Devak and Dhanya et al. 2014; Pervez and Henebry 2014).

There are number of literatures which has emphasized on the future climate prospects of India region where statistical downscaling has been used as an implicit technique (Tripathi et al. 2006; Salvi et al. 2011; Salvi and Ghosh 2013; Shashikanth et al. 2014; Shashikanth and Sukumar 2017). In a sub-regional context, several statistical and dynamic downscaling based studies has reported possible changes of minimum, maximum and mean temperature as well as men rainfall during different scale (i.e. Monthly, Seasonal and Annual), different time period (2020s, 2050s, and 2080s) and in different regions of Himalaya (Shrestha and Devkota 2010, Kulkarni et al. 2013, Mahmood and Babel 2013, Wiltshire 2014, Singh et al. 2015, Sharma et al. 2015, Rajbhandari et al. 2016, Sanjay et al. 2017, Altaf et al. 2017, Akhter 2017, Arya and Prasad 2017, Parvaze et al. 2017). A brief literature review on downscaling of rainfall and temperature over different regions of Himalaya has been provided in Table 1. All the trilogy of maximum temperature (Tmax), minimum temperature (Tmin) and mean temperature (Tmean) projected to increase over the Himalayan region under different climate change scenarios. On the other hand, projected mean rainfall may diminish or intensify during a different period of 21st century.

Rainfall over the WHR is highly localized and is influenced by complex topography and large-scale circulations like summer monsoon and western disturbances (Meher et al. 2017; Meher et al. 2018). Performance of CMIP5 GCMs over the WHR has shown improvement over CMIP3 GCMs in simulating the mean, interannual variability and short-term trend of observed rainfall data (Meher et al. 2017). Improvement in the skill of GCMs across generation is a positive sign towards our advanced understanding of various parameterization schemes employed in the GCMs. Hence; they must be incorporated in the downscaling studies for a better understanding of the future climate of the region. A local scale statistical downscaling study over

the WHR incorporating a multi-model approach was missing in the literature. In addition, earlier studies as mentioned in Table 1 only examined a specific portion of the WHR or a very large area, of which WHR is a tiny part. Hence, to bridge these research gaps present study has been attempted to meet the following objectives.

- To develop and validate multiple stations specific statistical downscaling models over the WHR.

- To construct local future annual and seasonal precipitation scenarios from existing CMIP5 GCMs using empirical statistical downscaling techniques over the Western Himalayan Region (WHR) of India.

2. Study region and data used

2.1. Study region

The study region is a part of Hindu Kush Himalaya (HKH) region consists of two north India states – Himachal Pradesh and Uttarakhand as shown in figure 1. Geographically it is located between 28°42´–33°12´N and 75°40–81°-50´E. One of the major rivers of India – 'The Ganga' originates from the Gangotri glacier located in the Uttarakhand state. This region is a part of greater Himalayan mountain range comprising an area of 1092.39 km^2 (i.e. ~ 20.45% geographical area of the Indian Himalayan region). Glaciers present in the high topographic of this region, feeds water to most of the rivers (e.g. The Chenab, The Yamuna, The Chandra, The Mandakini, The Pindari, The Ramganga, The Goriganga) flowing in Northern India. The local relief of the study region varies from 210 to 7817m above mean sea level. The high altitude locations of this region are mostly cold deserts and record low annual rainfall compared to the foothills. Lahul & Spiti region of Himachal Pradesh, and a very small pocket in Garhwal beyond Badrinath and Neelang Region in Uttarkashi districts of Uttarakhand state falls under the cold deserts. The climate of the study region is mostly dry to semi-humid; snowfall over this region starts during December and continues to March. The rainfall over this region is highly erratic and is affected by Indian monsoon during June to September, WD during December to Early March and El Niño-Southern Oscillation (ENSO) (Meher et al. 2017; Meher et al. 2018).

2.2. Data used

2.2.1. Observational Data or Predictand

Twenty-two number of rain gauge stations (eight in Himachal Pradesh and fourteen in Uttarakhand) having monthly rainfall during the period 1901-2005 were taken in the present study (However 1950-2005 time period was used for this study as a common time window for all the dataset). These were considered as the reference stations having long-term rainfall data procured from the India Meteorological Department (IMD) and was extensively used in the earlier studies (Meher et al. 2014; Meher et al. 2017; Meher et al. 2018 and Meher and Das 2018) for the purpose of climate change and GCM evaluation studies. IMD high resolution (0.25 × 0.25 latitude-longitude) gridded data developed by Pai et al. (2014a, 2014b) were used to fill the missing values in the mean monthly rainfall data. A detailed description of the missing value substitution in the original monthly rainfall data can be accessed from Meher et al. (2017) and Meher and Das (2018). The location details of the rain gauge stations taken in this study have been provided in Table 2.

2.2.2. Large-scale fields or Predictors

Large-scale predictors taken for the present study were given in the Table 3 which comprise of ten GCMs from the Coupled Model Intercomparison Project phase 5 (CMIP5) and four reanalysis predictors from the NCEP/NCAR. The GCMs and the reanalysis data used are open source and can be downloaded from the web link of the Lawrence Livermore National Laboratory archives (https://esgf-node.llnl.gov/projects/esgf-llnl/) and the archives of Earth System Research Laboratory (ESRL) of National Oceanic and Atmospheric Administration (NOAA) https://www.esrl.noaa.gov/psd/data/gridded/data.ncep.reanalysis.html respectively. The reanalysis predictors were developed by the National Centers for Environmental Prediction/National Center for Atmospheric Research (NCEP/NCAR) (Kalnay et al. 1996). Two parameters viz. monthly mean of relative humidity at 500 hPa (rhum500) and monthly precipitation (pr) for the GCMs as well as the reanalysis data were taken in this study. NCEP data don’t contain ‘precipitation’ as a parameter while precipitation rate (unit: mm/day) was converted to monthly precipitation (unit: mm/month) for the present study.

The first ensemble runs having single initialization states and physical parameterization (r1i1p1) scheme was considered for the GCM datasets. All the GCMs and NCEP simulations containing monthly rainfall data during the period 1950-2005 were retrieved from their respective achieves while the future data for the GCMs were retrieved for a common period of 2006-2095 under RCP4.5 scenario.

In the present study June to September was considered as the monsoon season and December to February was considered as the winter season.

3. Methodology

Stepwise method for statistical downscaling used in this study is described below. The downscaling involved were carried out for three different time scale i.e. Annual, monsoon (June, July, August, September) and winter (December, January, February). In case of annual time scale, the total rainfall was used for downscaling, where as in monsoon and winter season, the mean monthly rainfall was downscaled.

Step 1: Common resolution of all data sets:

The horizontal resolutions of all the datasets were converted to a common grid resolution of 1.5°×1.5° to avoid any systematic bias in the results. The selection of the common resolution depends on the choice of user as per the original resolution of the datasets taken.

Step 2: Selection of Predictand:

Twenty two number of observational IMD rain-gauge station having rainfall data during 1950-2005 were selected as predictands on the basis of our previous investigations (Das et al. 2018)

Step 3: Selection of predictor domain and predictors:

This is the crucial step of statistical downscaling process. In this step, firstly suitable predictor/s from the reanalysis data was selected based on either literature review or a descriptive statistical

analysis as done in our earlier study (Das et al. 2018). Later on, the same predictor parameters from the GCMs were taken to employ them in the downscaling process.

Initially, a very larger domain of South Asia (10° S-40° N, 20°-120° E) was taken to see the spatial correlation i.e. the correlation between observational data and the predictor data at each grid (using annual as well as seasonal data). The region where the spatial correlations were maximum was taken as the predictor domain (Das et al. 2018). For the present study, a larger area between 27-38° N and 72-82° E around the study region was considered as the predictor domain as described in our earlier study (Das et al. 2018).

In the same study, the selection of suitable predictor over the study domain in annual, monsoon (June to September) and winter (December to February) time scale was carried out using twenty four number of potential predictors from the NCEP/NCAR reanalysis data. Das et al. (2018) basically used two different skill score to select the performance of predictor. The skill scores were:

a. Adjusted R^2 of multiple regression between the 7-leading Empirical Orthogonal Function (EOF) of predictor and regional averaged observational data.
b. Correlation between the regional average data of the observation and the predictors.

Finally, the ranking of all the predictors for a particular season was carried out using their skill score values. The top ranked predictor was used as a suitable predictor for the downscaling study. After the selection of suitable predictors from the reanalysis data, the same predictor parameters must be taken from the GCM simulations and scenarios runs.

Step 4: Model setup and calibration:

The model setup was carried out using a combined EOF of the gridded reanalysis data and the GCM data as predictor while rain gauge data as the predictand as suggested by Benestad (2001b).

In this approach, the time series from reanalysis and GCM data represent exactly the same spatial pattern. Here the two data fields with data points on a common grid are combined along the time axis (concatenated), and an EOF analysis is applied to the combined dataset.

The EOF analysis is applied to the anomalies from the respective GCM and reanalysis climatologies. Each of the predictands and each grid box values of the reanalysis data were detrended (i.e. original value minus the linear trend values) to reduce systematic bias towards the model calibration (Benestad, 2001a).

Singular value decomposition (SVD) was used to calculate the EOFs used in this study. The EOFs used were estimated from a subsample of the data to avoid temporal autocorrelation, and the principal components have then been calculated according to the following inequality.

$$\mathbf{V^T = (A^T A)^{-1} A^T U^T X}$$

Where, X, U, A, and V represents the data field (anomalies), EOFs, diagonal matrix of eigenvalues, and principal components respectively. Here all the well resolved EOFs were mutually orthogonal ($\mathbf{U^T U=I}$) and any spatial anomaly pattern will therefore be a specific combination of EOFs.

A statistical model describing the relation between predictors (x) and predictands (y) can be written as

$$\boldsymbol{y=\Omega(x)}$$

Here $\boldsymbol{\Omega}$ represents the statistical model, which was obtained by treating $\boldsymbol{x}$ be the principal components of the predictors used for model development and $\boldsymbol{y}$ be the IMD station rainfall record and then solving for $\boldsymbol{\Omega}$. The empirical downscaling models used in this study were developed using canonical correlation analysis.

All these model types were trained with the 10 leading common EOFs through stepwise screening calibration (Wilks, 1995; Kidson and Thompson, 1998), in which the contribution of

each predictor was evaluated through a cross-validation analysis (Wilks, 1995). Only those that contributed to the cross-validation skill were included in the predictor dataset.

Different statistical skill scores like Perkin score (Perkin et al. 2007), mean error or mean bias and normalized root mean squared error (NRMSE) were used to calibrate the model over a 30-year window of 1951-1980. A short description of each matrices has been given below.

- **Perkin score (P):**

This index (P) calculates the cumulative minimum value of two different distributions of each binned value. As a result, it calculates the common area between two probability distribution functions (PDFs). Values of P or total sum of the probability at each bin center in a given PDF lie between 0 and 1. P=1 represents the distribution of model and the observations are perfectly similar i.e. both the distributions overlap each other. While, P=0 represents the model and the observed distributions are unique in their own way. The perkin score is given by,

$$\textbf{Perkin Score, } P = \sum_{i=1}^{n} minimum\left(Z_m, Z_O\right)$$

Where, n, Z_m, and Z_O represents the number of bins used, frequency of values in a given bin from the model, and frequency of values in a given bin from the observed rainfall data respectively.

- **Normalized Root Mean Squared Error (NRMSE)**

NRMSE is a measure of error when there exists a distinct difference between the observed data and the model data. Here the normalization was achieved using the observed data set. The normalization factor depends on the choice of user, while common choices are the mean, standard deviation or the range of the measured data. A lower NRMSE values indicate less residual variance. NRMSE is scale-dependent and is sensitive to outliers. The expression for NRMSE is as follows

$$\mathbf{NRMSE} = \frac{100}{\sigma_0}\left[\frac{1}{N}\sum_{i=1}^{N}(M_i - O_i)^2\right]^{1/2}$$

Here, the standard deviation of observation (σ_o) was used for normalization. M represents the Model generated values, O is the observed values, N, is the length of common time window of modeled and observed data.

- **Mean error (me)**

Mean error is the measure of average bias between the model and the observed datasets. It is expressed as

$$\mathbf{me} = \frac{1}{N}\sum_{i=1}^{N}(M_i - O_i)$$

Here, M represents the Model generated values, O is the observed values, N, is the length of common time window of modeled and observed data.

Step 5: Model validation:

The same statistical skill scores as mentioned above were also used to validate the model over a 25-year window of 1981-2005. In this step, the unused data from the GCMs during the period 1981-2005 were used in the model developed in step 4.

Step 6: Construction of future precipitation scenarios

The same model developed in step 4 was used to project the GCM data during the three different 30-year time windows of 2006-2035, 2036-2065, and 2066-2095. The scenario data of the GCMs were used to downscale the local precipitation at each of the rain gauge stations taken in the study.

Both mean rainfall (at annual, monsoon and winter time scale) and standard deviation of rainfall for each month (or the annual cycle of standard deviation) were downscaled at each of the station location using the method mentioned above.

4. Results and discussion

The suitable predictor selected to downscale annual and monsoon rainfall during the period 1950-2005 was precipitation rate (pr), while relative humidity at 500 hPa (rhum500) was the best predictors during the winter season over the selected domain. These were the predictors, which acquired top rank among the twenty-four predictors taken in our earlier study (Das et al. 2018). The reason for getting two different predictors in the study region is, there exists two distinct seasons in the study region with distinct characteristics of prevailing circulation patterns. During monsoon season, the study region gets ~80% of the annual rainfall (1250.1 ± 241.7mm) from the large scale Southwest monsoon, while ~11% of the annual rainfall was received during the winter season from the eastward flowing western disturbances (Meher et al. 2017). In connection to relative humidity parameter, it was shown in the literatures that, zonal and meridional structures of the relative humidity was an important parameter of the vertical structure of Western Disturbances (Hunt et al. 2018) and can be taken as parameter to simulate the precipitation and circulation pattern of the western disturbances in the model evaluation studies (Azadi et al. 2002; Thomas et al. 2018).

4.1. Performance of predictors during calibration

Figure 2 shows the performance hur500 and Pr predictors for all the 22 number of rain gauge stations using different skill scores viz. Perkin score, Mean error and NRMSE during the time calibration time period 1951-1980 in the monsoon and winter season. The predictor ‘hur500’ was originally selected to downscale the winter precipitation and ‘Pr’ for monsoon precipitation, none the less both the predictors were used to calibrate the downscaled model to verify whether any of them is redundant (i.e. redundancy of Pr in winter season and hur500 in monsoon season). This is a simple assumption, which can be solved through the analysis of agreement and error indices used in the study. The skill scores for a particular station represented the ensemble mean skill scores of all the GCMs. The skill scores of calibration period for the annual time scale were not shown, as they were same as the monsoon season.

4.1.1. Analysis of Perkin Score

The mean value of the agreement index i.e. the 'Perkin score (P)' in monsoon season, was ~0.50 for both the predictors. $0.70 \geq P \geq 0.50$ for stations like Banjar, Berinag, Dehra Gopipur, Hamirpur, Karnaprayag, Kasauli, Kashipur, Nurpur, Rajpur, and Ramnagar. Similarly $0.50 \geq P \geq 0.40$ for stations like Haldwani, Kangra, Kathgodam, Kotdwara, Kotkhai, Lansdowne, Palampur and Srinagar. The P values for all the stations were >0.35 except Ranikhet. In winter season the mean value of Perkin score (P) were ~0.45 for both the predictors. All the stations showed the value of $0.6 \geq P \geq 0.35$ during the winter season. The result showed that downscaled PDFs of the monsoon season precipitation for most of the stations were quite similar to the observed PDFs where as in winter season their performances were nominally lower than the Monsoon season. Calculated P values for both the predictor failed to explain the redundancy assumption proposed in the earlier paragraph.

4.1.2. Analysis of mean error

The mean value of error index i.e. the 'mean error (me)' in monsoon season was ~4.62 for the 'pr', whereas it was higher for the hur500 (me ~ 29). The mean error shown by 'pr' was ~ 0 for most of the stations like Almora, Berinag, Bironkhol, Hamirpur, Kathgodam, Kotdwara, Lansdowne, Okhimath, Palampur, Ramnagar, Ranikhet, and Srinagar. Notable differences can be seen between the mean error values of the two predictors (me of hur500 > me of pr) in some stations like Dehra Gopipur, Kangra, Nurpur, Palampur, Rajpur, and Srinagar. In winter season, the mean value of me was ~14 for the 'hur500', whereas it was higher for the pr (me ~ 55). The mean error shown by 'hur500' was ≤ 7 for the stations like Almora, Banjar, Berinag, Kangra, Kotkhai, Nurpur, Okhimath, Palampur, Rajpur, and Ranikhet. Notable differences can be seen between the mean error values of the two predictors (me of pr > me of hur500) in all the stations over the study region. Overall the results showed that during the calibration period, the selected 'suitable predictors' for the monsoon (pr) and winter (hur500) season showed very nominal bias of downscaled precipitation with the observed precipitation, whereas notable and higher bias were seen between the downscaled and observed precipitation during monsoon and winter season using hur500 and pr as predictors respectively. Hence the assumption of hur500 can be

taken also as a suitable predictor to downscale monsoon and annual precipitation; and pr can be taken as a suitable predictor to downscale winter precipitation is false. Nonetheless trueness of this statement was also tested in the following paragraph using the NRMSE as another error index.

4.1.3. Analysis of Normalized Root Mean Squared Error.

The mean value of another error index i.e. the ‘Normalized Root Mean Squared Error (NRMSE)’ in monsoon season was ~75 for the ‘pr’, whereas it was higher for the hur500 (me ~ 79). The NRMSE values shown by ‘pr’ was < 65 for some stations like Kangra, Lansdowne, Okhimath, Palampur, and Rajpur. Notable differences can be seen between the NRMSE values of the two predictors (NRMSE of hur500 > NRMSE of pr) in some stations like Haldwani, Kangra, Kotdwara, Lansdowne, Nurpur, Okhimath, Palampur, and Rajpur. In winter season, the mean value of NRMSE was ~85 for the ‘hur500’, whereas it was higher for the pr (me ~ 90). The calculated NRMSE values shown by ‘hur500’ was ≤ 80 for the stations like Kasauli, Okhimath, and Ranikhet. Notable differences can be seen between the NRMSE values of the two predictors (NRMSE of pr > NRMSE of hur500) in some stations over the study region like Berinag, Bironkhol, Karnaprayag, Kathgodam, Nurpur, Okhimath, Ramnagar, and Srinagar. Overall the results showed that during the calibration period, the selected ‘suitable predictors’ for the monsoon (pr) and winter (hur500) season showed lower normalized error values between the downscaled precipitation and the observed precipitation, whereas notable and higher normalized error were seen between the downscaled and observed precipitation during monsoon and winter season using hur500 and pr as predictors respectively. In addition, the assumption of hur500 can be taken also as a suitable predictor to downscale monsoon and annual precipitation; and pr can be taken as a suitable predictor to downscale winter precipitation is false. Hence, the trueness of this statement holds also using NRMSE as a skill score to evaluate the performance of both the predictors during the calibration period.

4.2. Validation results

Figure 3 shows the performance of individual GCM predictors during the validation period of 1981-2005 using the skill scores (P, me, and NRMSE). The GCM outputs of predictor 'pr' were used in the downscaled model for annual and monsoon precipitation, whereas the GCM outputs of predictor 'hur500' were used in the downscaled model for the winter precipitation. Calculated values of the skill scores for all the 22 stations were used to generate the box plot for the GCMs.

4.2.1. Validation from Perkin Score

The calculated value of Perkin score (P) values in annual time scale were, $0.60 \geq P \geq 0.24$ for all the GCMs. Except seven stations - Kashipur, Kotdwara, Lansdowne, Palampur, Rajpur, Ramnagar, and Srinagar all the other stations showed P values >0.42 in most of the GCMs. Banjar, Kathgodam and Okhimath stations have shown P>0.55 for all the GCMs. Four GCMs (BNU-ESM, CMCC-CMS, MPI-ESM-LR, and NorESM1-ME) were the better performing GCMs having the median value of P ~ 0.45. In the monsoon season the P values were $0.54 \geq P \geq 0.26$ for all the GCMs. In this season, all the stations except Berinag, Bironkhol, Palampur, Ramnagar, and Srinagar have shown P values >0.40 in most of the GCMs. The calculated values of P for six stations - Banjar, Dehra Gopipur, Karnaprayag, Kotkhai, Lansdowne, Nurpur, and Okhimath were ~0.48 during the monsoon season. Most of the GCMs (except BNU-ESM and NorESM-ME) were the better performing GCMs in this season having a median value of P ~0.40. In winter season the P values were, $0.51 \geq P \geq 0.20$ for all the GCMs. All the statins except Bironkhol, Haldwani, Kashipur, Palampur, and Ramnagar have shown P values ≥0.30 in most of the GCMs. Three stations ─ Banjar, Karnaprayag, and Okhimath have shown P values ~0.40 in all the GCMs during the winter season. The median value of P for four GCMs were bcc-csm1-1-m, CNRM-CM5, MPI-ESM-MR, and NorESM1-ME were ~3.2, however with a P value of 3.6 MPI-ESM-MR was the best GCM in winter season.

The above validation results based on Perkin score revealed that precipitation distribution during the validation period were similar to the observed distribution up to some extent in some stations like Banjar, Karnaprayag, Kotdwara, Lansdowne, Okhimath, Rajpur, and Srinagar as

these stations shown Perkin score between 0.40-0.55 irrespective of time scale. One of the most notable features of rainfall distribution in the study region during the period 1951-2005 was, there was a sudden shift of rainfall in most of the stations during 1960-70. As a result, the rainfall distribution, before 1960-70 and after 1960-70 were different from each other (Basistha et al. 2009, Kumar and Jaswal 2016, Meher et al. 2017, Meher et al. 2018). This may be a possible reason for Perkin score in validation period were less than the calibration period.

4.2.2. Validation from Mean error

It was revealed that calculated value of mean error (me), were almost similar for all the GCMs in individual time scale. In the annual time scale the median value of the mean error were ~80. Stations like Bironkhol, Karnaprayag, Haldwani, Kashipur, Kathgodam, Lansdowne, Nurpur, and Ramnagar have shown a mean error value ~ 130 in all the GCMs. Whereas, stations like Almora, Banjar, Berinag, Dehra, Gopipur, Kangra, Kasauli, Okhimath, Ranikhet, and Srinagar have shown a very low mean error value of ~21 to 27. Highest mean error (~231) was seen in the Rajpur and Kotdwara stations in most of the GCMs. CanESM2 was the best performing GCM with a median value of the mean error ~72. In the monsoon season the median value of the mean error were lies between 26-38 in all the GCMs. Stations like Haldwani, Karnaprayag, Kashipur, Kotdwara, Kotkhai, and Nurpur have shown a mean error value in the range 45-76 in all the GCMs. Whereas, stations like Almora, Berinag, Dehra Gopipur, Kangra, Kasauli, and Srinagar have shown a very low mean error value between -10 and 10. Higher mean error values was seen in the Palampur, and Rajpur stations in most of the GCMs with a mean value of ~ -109 and 140 respectively. Five stations viz. Hamirpur, Kangra, Kasauli, Palampur, and Srinagar have shown a dry bias in all the GCMs with a range of -10 to 0 (-109 in Palampur). CanESM2 was the best performing GCM with a median value of the mean error ~13. In winter season the mean error values were very less with a median value < 6 in all the GCMs. Three stations namely Bironkhol, Nurpur, and Okhimath have shown higher mean error values (~18) in all the GCMs compared to other stations. Some stations over the study region viz. Almora, Banjar, Berinag, Haldwani, Hamirpur, Kathgodam, Palampur, Ranikhet, and Srinagar have shown nominal wet bias (-1 to -11) with respect to the observed rainfall. The performance of all

the GCMs were quite similar to each other, however the NorESM-ME GCM with a median value of the mean error ~2 was the best performing GCM during the winter season.

The above validation results based on mean error showed an decreasing order of Mean error values in different time scale is, me in annual time scale > me in monsoon > mean error in winter season during the validation period. The reason for higher mean error in annual is the higher magnitude of rainfall received in annual where as in winter the rainfall received over the study region were lower.

4.2.3. Validation from Normalized Root Mean Squared Error

Like the mean error, calculated values of NRMSE were also similar for all the GCMs in individual time scale. In the annual time scale the median value of the NRMSE were ~40. Stations like Berinag, Kasauli, Nurpur, Palampur, and Rajpur have shown a NRMSE value lying between 70 and 80 in all the GCMs. Whereas, stations like Almora, Dehra Gopipur, Hamirpur, Kathgodam, Kotkhai, Ranikhet, and Srinagar have shown a very low NRMSE value lying between ~25 and 35. Highest NRMSE (~80) was seen in the Rajpur and Berinag stations in most of the GCMs. NorESM1-M was the best performing GCM with a median value of the NRMSE ~39. In the monsoon season the median value of the NRMSE were lies between 91-98 in all the GCMs. Stations like Haldwani, Kashipur, Kotkhai, and Ramnagar have shown a NRMSE value in the range 102-119 in all the GCMs whereas stations like Dehra Gopipur, Hamirpur, Kangra, Lansdowne, and Okhimath have shown a lower NRMSE value between 86 and 89. Higher NRMSE values was seen in the Kotkhai and Ramnagar stations in most of the GCMs with a mean value of ~ 110 and 119 respectively. NorESM1-M was the best performing GCM with a median value of the NRMSE ~91. In winter season the NRMSE values were < 109 in all the GCMs. Four stations namely Bironkhol, Karnaprayag, Nurpur, and Ramnagar have shown higher NRMSE values (between 112 and 115) in all the GCMs compared to other stations. CanESM2 and MPI-ESM-LR GCMs were the better performing GCMs with a median value of ~101.5 during the winter season.

4.3. Analysis of projected mean precipitation

The model that was developed by the combined EOF approach of the GCMs and reanalysis gridded predictors during the historical period was used for the future projection of rainfall in each of the stations. The RCP4.5 scenario data generated during annual, monsoon and winter time scale from each GCM was used in the calibration model to find out the change of rainfall during the 21st century. Three sub-periods viz. 2006-2035 (2020s), 2036-2065 (2050s) and 2066-2095 (2080s) were considered to calculate the percentage change of rainfall in the future. Table 4 shows the % change (Δ) of 95th percentile estimates of rainfall during different sub periods viz. 2020s, 2050s and 2080s in the 21st century calculated from the downscaled ensemble mean of ten GCMs (MME10). The historical time period of 1951-2005 was used as the baseline to calculate the % change of rainfall in each of the sub-periods. Earlier studies on the CMIP5 model evaluation by Palazzi et al. (2015) highlighted that no single CMIP5 model (out of 32 models) provides the best simulation in precipitation, and the large spreads of individual models suggest to consider multi-model ensemble means approach to study past and future climate change over the Hindu Kush Himalayan region. This was the reason we considered to limit our analysis of future projection of precipitation using the multi model ensemble approach.

4.3.1. Change of rainfall in annual time scale

Table 4 revealed that there would be surplus of rainfall in most of the stations (i.e. 18 out of 22 stations) in the study region during different sub-periods of 2020s, 2050s, and 2080s. In addition, there were few stations viz. Karnaprayag, Kasauli, Lansdowne, and Rajpur that may face a deficient rainfall during all the sub-periods. A peculiar nature of positive/negative percentage change in rainfall (Δ) was noticed in most of the rain gauge stations of the study region where $\Delta_{2020s} > \Delta_{2050s} > \Delta_{2080s}$. Whereas in few stations like Almora, Berinag, Dehra Gopipur, Hamirpur, Kotdwara, Palampur, and Srinagar the opposite trend of rainfall change was noticed i.e. $\Delta_{2020s} < \Delta_{2050s} < \Delta_{2080s}$. The stations, which recorded a surplus of rainfall in future, have a mean Δ of 8.9 % in 2020s, 7.7 % in 2050s, and 6.5 % in 2080s. Similarly the stations which recorded a deficient rainfall in future have a mean Δ of – 12.0% in 2020s, -10.9% in 2050s and -4.5% in 2080s. Nominal change in Δ (i.e. 0.2% to 3%) was observed in stations like

Almora, Berinag, Kangra, and Ranikhet. Stations like Bironkhol, Haldwani, Kashipur, Kotdwara, and Nurpur may receive 10-16% surplus rainfall in different sub-periods. Ramnagar station may face the highest change of rainfall i.e ~ 25-29% more rainfall during 2006-2065. On the other hand, in Karnaprayag and Rajpur stations may face an acute deficit of rainfall during the 21st century, which ranges from -9 to -14% and -9 to -22% respectively. Overall analysis of projected rainfall change in annual time scale revealed a wetter climate in the future in most of the locations of the study region under a changing climate with highest radiative forcing scenario of RCP4.5.

Earlier studies on the change of annual rainfall in 21st century through statistical downscaling approaches reported an wetter climate in different portions of Western Himalaya region like Sutlej river basin (Singh et al. 2015), Jhelum river basin (Mahmood and Babel 2013), Lidder river basin (Altaf et al. 2017) and different districts of Uttarakhand (in the monthly time scale) (Sharma et al. 2015). Panday et al. (2015) analyzed the simulated and projected precipitation over the western Himalaya-Karakoram using the CMIP3 and CMIP5 models. They also reported a wetter climate during the future over the study region. On the other hand, model evaluation study by Wu et al. (2017) reported that future precipitation is projected to increase over most part of Hindu Kush Himalaya region, except for the northwestern part.

4.3.2. Change of rainfall in monsoon season

In monsoon season the projected rainfall at majority of the stations may increase with respect to the base line period. There are few stations (Hamirpur, Karnaprayag, Kasauli, Lansdowne, and Rajpur) where the projected rainfall revealed a deficit in all the sub-periods. Majority of the stations (12 out of 22 stations) namely Bironkhol, Kangra, Karnaprayag, Kasauli, Kathgodam, Kotkhai, Lansdowne, Nurpur, Okhimath, Rajpur, Ramnagar, and Ranikhet over the study region have shown a decreasing trend of Δ across the three sub-periods i.e. $\Delta_{2020s} > \Delta_{2050s} > \Delta_{2080s}$. On the other hand, in some stations like Almora, Berinag, Dehra Gopipur, Haldwani, Hamirpur, Kashipur, and Kotdwara the peculiar trend of increasing rainfall (as seen in the annual time scale) was also seen across the different sub-periods i.e. $\Delta_{2020s} < \Delta_{2050s} < \Delta_{2080s}$. The stations, which recorded a surplus of rainfall in future have a mean Δ of 10.4 % in 2020s, 11.2 % in

2050s, and 10.1 % in 2080s. Similarly the stations which recorded a deficient rainfall in future, have a mean Δ of – 17.6 % in 2020s, -11.32% in 2050s and -11.37 % in 2080s. Comparisons between the average value of percentage changes in annul and monsoon projected rainfall of all the stations showed a clear different between the two i.e. $\Delta_{Monsoon} > \Delta_{Annual}$ during all the sub-periods. Which represented the south-west monsoon rainfall may intensify in future climate over the study region. The percentage change of rainfall in some stations like Nurpur, Okhimath, Palampur, and Ramnagar have shown a higher value i.e. ~14-21.5% during the first two sub-periods (i.e. 2020s and 2050s) compared to all the other stations. Rajpur station has shown the highest deficit of rainfall among all the stations with a Δ value of ~30% in 2020s and ~18% in the 2050s. Kangra, Kasauli, and Kathgodam stations have shown a nominal change in rainfall having a Δ of 1.66% to 3.71%, -1% to -2.5% and 1.7% to 6.8% respectively in future. Overall analysis of projected rainfall change in monsoon season revealed a wetter climate in the future in most of the locations of the study region under a changing climate with highest radiative forcing scenario of RCP4.5.

Thermal contrast between the Tibetan plateau and the India ocean act as an active driver of south-west monsoon rainfall over the India region resulted in transportation of water vapor from the tropical Indian Ocean to the Himalayas (Duan et al. 2006; Meher et al. 2017). A higher monsoon rainfall in future may be attributed to the strengthening of the thermal contrast between the two regions of the earth in future. In relation to future projection of monsoon rainfall over the study region, Kulkarni et al. (2013) reported that summer monsoon precipitation is expected to be 20–40% higher in 2071–2098 than it was in the baseline period (1961–1990) over the Hindu Kush Himalayan region. Their findings were based on the study of high-resolution Regional Climate Model PRECIS (Providing Regional Climates for Impact Studies). Palazzi et al. (2013) also reported an increase in projected monsoon season mean precipitation with an increase in heavy rainfall days over the Hindu-Kush Karakoram Himalaya using single CMIP5 model simulation. Kadel et al. (2018) recently studied the projection of future monsoon precipitation over the central Himalayas (including the present study region) by 38 CMIP5 GCMs. Their study reported an increase in summer monsoon mean precipitation in all future periods under RCP4.5.

4.3.3. Change of rainfall in winter season

Downscaled precipitation projections in the winter season have shown opposite characteristics of what annual and monsoon precipitation projections were expected to show in future in the study region. Which means that, climate in the winter season over the study region is expected to be drier as all the stations revealed a deficient rainfall in all the three sub-periods of 2020s (exception Kotdwara and Bironkhol stations), 2050s and 2080s. Like precipitation projection in monsoon season and annual time scale, in winter season also an increasing nature of mean percentage change of rainfall in future was observed across the three sub-periods i.e. $\Delta_{2020s} < \Delta_{2050s} < \Delta_{2080s}$. The lowest decrease is expected during the 2020s with a mean Δ value of -2%, whereas in 2050s and 2080s the calculated values of Δ was -10.4 % and -19.2 % respectively. Stations with highest value of declining Δ of winter precipitation were Dehra Gopiur in 2020s (Δ=-3.4%), and Kotkhai in 2050s and 2080s (Δ= -15.4%, and -28.4% respectively). The stations which are expected to face higher precipitation deficit (Δ > 12.5%) during 2050s are Dehra Gopipur, Kasauli, Kotkhai, Okhimath, Rajpur, and Ramnagar. Similarly, the stations which are expected to face higher precipitation deficit (Δ > 25%) during 2080s are Kasauli, Kotkhai, Okhimath, and Ramnagar. Overall analysis of winter rainfall projection from the downscaled data revealed that study region is expected to get deficient precipitation in 21st century under a changing climate with highest radiative forcing scenario or RCP4.5.

Precipitation in the study region during the winter season is mainly attributed to the passage of eastward flowing western disturbances, which tend to develop over the Mediterranean Sea and Atlantic Ocean. Decrease in the winter precipitation may be directly linked to the decreasing frequency of western disturbances in future.

4.4. Analysis of the projected uncertainty of precipitation

Figure 4 shows the downscaled standard deviation of monthly precipitation in all the stations locations during different sub-periods in future. Both the predictors were used to downscale the standard deviation of precipitation but the findings of predictor ‘pr’ were only included in the text as both of them shown very similar results.

Hasson et al. (2016) reported that reliability of climate model's projections for future changes in the hydrology of South and South East Asia region largely depends upon their realistic representation of both monsoon precipitation regime and the westerly precipitation regime for the present-day climate. In figure 4, the downscaled results show a realistic representation of the standard deviation of precipitation in all the months. Most important features of the figure 4 were, the monsoon precipitation regime and the winter/westerly precipitation regime were well reproduced through downscaling method. The amplitude of standard deviation (σ) values in different sub-periods has shown a distinct pattern of increasing trend from 2020s to 2080s i.e. σ2020s < σ2050s < σ2080s in ten out of twelve month (January, February, March, April, May, June, September, October, November, December). In July and August months, the increasing pattern of standard deviation was σ2050s < σ2020s < σ2080s and σ2050s < σ2080s < σ2020s respectively. The inclining trend of standard deviation across the different sub-periods represented an increasing uncertainty of projected precipitation with the progress of time. Results also showed five classes of standard deviation values (average value of σ of all the stations) i.e. 0-50 in November and December; 51-100 in January, February, March, April, and October; 101-150 in May, June and September; 151-200 in July, and 201-250 in August. The higher value of standard deviation in July and August month and an unfamiliar trend as discussed above represents that peak monsoon months were associated with random uncertainty in future. The stations, which may face higher uncertainty of winter month's rainfall in future are Dehra Gopipur, Kasauli, Nurpur, Palampur, and Hamir. Similarly, the uncertainty of monsoon month's rainfall is expected to be higher in stations like Berinag, Dehra Gopipur, Haldwani, Kasauli, Kathgodam, Nurpur, Palampur, and Rajpur. In rest of the stations the uncertainty of rainfall is expected to be lower in winter and monsoon months. Palampur and Nurpur are the stations where the rainfall has consistently higher uncertainty in most of the months in the study region.

Month wise percentage change of 'average standard deviation values' of all the stations compared with the base line period showed that in seven out of twelve months viz., Jan, and March to August, there was a positive change of σ where as in Oct to December the change in σ was negative in all the sub-periods (figure 5). From figure 5 it is expected that later pre-monsoon months (dry seasons) and early post-monsoon month (dry season) will contributes maximum

uncertainty to the rainfall in the study region, which is followed by early post-monsoon month. However, this uncertainty may not impact the hydrological budget of the study region as rainfall during this time is very less in the past (<5% of annual rainfall) over the WHR (Meher et al. 2017; Meher et al. 2018).

5. Conclusion

Based on the results obtained from the present study the major conclusions were outlined as follows.

- Downscaled precipitation outputs from multi model ensemble of 10 CMIP5 GCMs under highest radiative forcing scenario of RCP4.5 revealed a wet climate in annual and monsoon, where as a dry climate is expected in future in the winter season over the Western Himalaya region.
- The total annual precipitation is expected to increase by 8.9 % in 2020s, 7.7 % in 2050s, and 6.5 % in 2080s compared to the baseline scenario. Similarly, mean monthly precipitation in the monsoon season may increase by 10.4 % in 2020s, 11.2 % in 2050s, and 10.1 % in 2080s. On the other hand, in the winter months the precipitation is expected to decline by 2% in 2020s, 10.4 % in 2050s and 19.2 % in 2080s.
- The downscaled standard deviation (σ) of monthly precipitation in different sub-periods has shown a distinct pattern of inclining trend from 2020s to 2080s which represents an increasing uncertainty of projected precipitation with the progress of time.
- Downscaled precipitation projection during the 21st century showed higher uncertainty of precipitation in pre-monsoon months (April and May) and early post-monsoon month (October) in the study region.

Acknowledgements

Jitendra Kumar Meher is thankful to Bidhan Chandra Krishi Viswavidyalaya for providing the basic lab facility to carry out the present work. The authors sincerely thank the Norway Research Council for funding the Indo-Norway international research project INDICE through which the

present work has been carried out. Authors would like to acknowledge IMD, Pune for providing the meteorological data used in the current research. The ESGF and NCEP/NCAR were duly acknowledged for their effort to making the GCM and reanalysis data publicly available for the present work.

Statements & Declarations

Funding

This work was supported by the fund received by Indo-Norway international research project INDICE. Jitendra Kumar Meher has received research support/fellowship from Norway Research Council during the preparation of the present work.

Competing Interests

The authors have no relevant financial or non-financial interests to disclose.

Ethics declarations

The authors understand their ethical responsibility towards the present submission. There is no violations to the ethics as mentioned by Springer publications.

Consent to participate

Not Applicable

Consent for publication

No published data were taken form any third person. Authors give their consent for publication of this article upon acceptance by the journal

Author Contributions

All authors contributed to the study conception and design. Data collection was done by Lalu Das. Material preparation and analysis were performed by Jitendra Kumar Meher. The first draft

of the manuscript was written by Jitendra Kumar Meher and Lalu Das commented on previous versions of the manuscript. Both the authors read and approved the final manuscript.

Code availability

The codes are available on resonable request

Data Availability

The observational data were procured from IMD-Pune, India. They will be made available on request. The datasets generated during and/or analysed during the current study are available from the corresponding author on reasonable request.

References

Akhter, M., 2017.Projection of future Temperature and Precipitation for Jhelum river basin in India using Multiple Linear Regression. Int. Journal of Engineering Research and Application, 6(4): 89-101

Altaf, Y., Ahmad, A. M., & Mohd, F. (2017). MLR Based Statistical Downscaling of Temperature and Precipitation in Lidder Basin Region of India. Environ Pollut Climate Change, 1(109), 2.

Arya, D.K., Prasad, H.J.S., (2017). Rainfall prediction for Roorkee (Uttarakhand) through statistical downscaling. Proceeding of the National conference on Advances in Water Resource and Environment Research, Centre for Remote Sensing and Geoinformatics, Sathyabama University, Chennai, 29-30 June 2017, pp 113-123.

Azadi, M., Mohanty, U. C., Madan, O. P., & Padmanabhamurty, B. (2002). Prediction of precipitation associated with a western disturbance using a high-resolution regional model: role of parameterisation of physical processes. Meteorological Applications, 9(3), 317-326.

Basistha A, Arya DS, Goel NK. 2009. Analysis of historical changes in rainfall in the Indian Himalayas. Int. J. Climatol. 29: 555-572. https://doi.org/10.1002/joc.1706.

Benestad RE. (2001a). The cause of warming over Norway in the ECHAM4/OPYC3 GHG integration. International Journal of Climatology 21: 371–387.

Benestad, R. E. (2001b). A comparison between two empirical downscaling strategies. International Journal of Climatology, 21(13), 1645-1668.

Benestad, R. E. (2010). Downscaling precipitation extremes. Theoretical and applied climatology, 100(1-2), 1-21.

Benestad, R. E. (2011). A new global set of downscaled temperature scenarios. Journal of Climate, 24(8), 2080-2098.

Benestad, R. E., Hanssen-Bauer, I., & Chen, D. (2008). Empirical-statistical downscaling. World Scientific Publishing Company: New Jersey, London.

Benestad, R. E., Hanssen-Bauer, I., & Førland, E. J. (2007). An evaluation of statistical models for downscaling precipitation and their ability to capture long-term trends. International Journal of Climatology, 27(5), 649-665.

Blazak, A. (2012). Statistical downscaling of precipitation projections in Southeast Queensland Catchments. Doctoral dissertation, University of Southern Queensland.

Chen, J., Brissette, F. P., & Leconte, R. (2014). Assessing regression-based statistical approaches for downscaling precipitation over North America. Hydrological processes, 2 (9), 3482-3504.

Das, L., Meher, J. K., & Dutta, M. (2016). Construction of rainfall change scenarios over the Chilka Lagoon in India. Atmospheric Research, 182, 36-45.

Das, L., Meher, J. K., Benestad, R. E., and Mezghani, A. 2018. Selection of suitable predictors and predictor domain for statistical downscaling over the Western Himalayan region of India. Climate research. (Submitted article)

Devak M, Dhanya CT (2014) Downscaling of precipitation in Mahanadi basin, India. International J Civil Eng Res 5:111-120.

Duan, K., T. Yao, and L. G. Thompson, 2006: Response of monsoon precipitation in the Himalayas to global warming. J. Geophys. Res., 111, D19110, doi:10.1029/2006JD007084.

Eden JM, Widmann M (2014) Downscaling of GCM-simulated precipitation using Model Output Statistics. J Climate 27 (1): 312-324. doi:10.1175/JCLI-D-13-00063.1

Ghawana, T., & Minoru, K. (2015) Indian Flood management: A report on Institutional arrangements. Integrated Spatial Analytics Consultants, Delhi, India & International Centre for Water Hazard and Risk Management (ICHARM) under the auspices of UNESCO; Public Works Research Institute (PWRI). Available at http://whrm-kamoto.com/assets/files/TARUN%20MINORU-ICHARM%20REOPRT%20ON%20INDIAN%20FLOOD%20MANAGEMENT%20INSTITUTIONS%20JANUARY%202015.pdf (Accessed on 30th May 2018)

Goyal MK, Ojha CSP (2010) Evaluation of various linear regression methods for downscaling of mean monthly precipitation in arid Pichola watershed. Natural Resources 1 (01): 11-18. doi:10.4236/nr.2010.11002

Hu Y, Maskey S, Uhlenbrook S (2013) Downscaling daily precipitation over the Yellow River source region in China: a comparison of three statistical downscaling methods. Theor. Appl. Climatol 112(3-4): 447-460. doi:10.1007/s00704-012-0745-4

Huang, J., Zhang, J., Zhang, Z., Xu, C., Wang, B., & Yao, J. (2011). Estimation of future precipitation change in the Yangtze River basin by using statistical downscaling method. Stochastic Environmental Research and Risk Assessment, 25(6), 781-792.

Hunt, K. M., Turner, A. G., & Shaffrey, L. C. (2018). The evolution, seasonality and impacts of western disturbances. Quarterly Journal of the Royal Meteorological Society, 144(710), 278-290.

Huth R (1999) Statistical downscaling in central Europe: evaluation of methods and potential predictors. Clim Res 13(2): 91-101.

Intergovernmental Panel on Climate Change (IPCC) (2013), Climate change 2013: The Physical Science Basis, in Contribution on Working Group I to the Fifth Assessment Report of the IPCC, edited by T. F. Stocker et al., 1535 pp., Cambridge Univ. Press, Cambridge, U. K., and New York

IPCC. 1995. The Second Assessment Report. Technical Summary, WMO & UNEP.

Kadel, I., Yamazaki, T., Iwasaki, T., & Abdillah, M. R. (2018). Projection of future monsoon precipitation over the central Himalayas by CMIP5 models under warming scenarios. Climate Research, 75(1), 1-21.

Kalnay E, Kanamitsu M, Kistler R, Collins W, Deaven D, Gandin L, Iredell M, Saha S, White G, Woollen J, Zhu Y (1996) The NCEP-NCAR 40-year reanalysis project. Bull Am Meteor Soc 77: 437-471. doi:10.1175/1520-0477(1996)077<0437:TNYRP>2.0.CO;2

Kannan S, Ghosh S (2013) A nonparametric kernel regression model for downscaling multisite daily precipitation in the Mahanadi basin. Wat Resour Res 49(3): 1360-1385. doi:10.1002/wrcr.20118

Kidson JW, Thompson CS. 1998. A comparison of statistical and model-based downscaling techniques for estimating local climate variations. Journal of Climate 11: 735–753.

Kulkarni, A., Patwardhan, S., Kumar, K. K., Ashok, K., & Krishnan, R. (2013). Projected climate change in the Hindu Kush–Himalayan region by using the high-resolution regional climate model PRECIS. Mountain Research and Development, 33(2), 142-151.

Kumar N, Jaswal AK. 2016. Historical temporal variation in precipitation over western Himalayan region: 1857–2006. J. Mt. Sci. 13: 672–681. https://doi.org/10.1007/s11629-014-3194-y.

Mahmood, R., & Babel, M. S. (2013). Evaluation of SDSM developed by annual and monthly sub-models for downscaling temperature and precipitation in the Jhelum basin, Pakistan and India. Theoretical and applied climatology, 113(1-2), 27-44.

Mahmood, R., & Babel, M. S. (2013). Evaluation of SDSM developed by annual and monthly sub-models for downscaling temperature and precipitation in the Jhelum basin, Pakistan and India. Theoretical and applied climatology, 113(1-2), 27-44.

Maraun D, Wetterhall F, Ireson AM, Chandler RE, Kendon EJ, Widmann M, Brienen S, Rust HW, Sauter T, Themeßl M, Venema VKC, Chun KP, Goodess CM, Jones RG, Onof C, Vrac M, Thiele-Eich I. 2010. Precipitation downscaling under climate change: Recent developments to bridge the gap between dynamical models and the end user. Reviews of Geophysics **48**(3). https://doi.org/10.1029/2009rg000314.

Meher, J. Das, L. 2018. Gridded data as a source of missing data replacement in station records. Journal of earth system science. (In press)

Meher, J. K., Das, L., & Akhter, J. (2014). Future rainfall change scenarios simulated through AR4 and AR5 GCMs over the Western Himalayan Region. *J. Agrometeor*, *16*, 53-58.

Meher, J. K., Das, L., Akhter, J., Benestad, R. E., & Mezghani, A. (2017). Performance of CMIP3 and CMIP5 GCMs to simulate observed rainfall characteristics over the Western Himalayan region. *Journal of Climate*, *30*(19), 7777-7799.

Meher, J. K., Das, L., Benestad, R. E., & Mezghani, A. (2018). Analysis of winter rainfall change statistics over the Western Himalaya: the influence of internal variability and topography. *International Journal of Climatology*, *38*, 475-496.

Nandargi, S., & Dhar, O. N. (2011). Extreme rainfall events over the Himalayas between 1871 and 2007. Hydrological sciences journal, 56(6), 930-945.

Ojha CS, Goyal MK, Adeloye AJ (2010) Downscaling of precipitation for lake catchment in arid region in India using linear multiple regression and neural networks. Int J Climatol 4(1): 122-136. doi:10.1002/joc.2286

Pai DS, Sridhar L, Badwaik MR, Rajeevan M. 2014b. Analysis of the daily rainfall events over India using a new long period (1901–2010) high resolution (0.25◦ × 0.25◦) gridded rainfall data set. Clim.Dyn. 45: 755–776. https://doi.org/10.1007/s00382-014-2307-1.

Pai DS, Sridhar L, RajeevanM, Sreejith OP, Satbhai NS, Mukhopadhyay B. 2014a. Development of a new high spatial resolution (0.25 × 0.25) long period (1901–2010) daily gridded rainfall data set over India and its comparison with existing data sets over the region.MAUSAM 65(1): 1–8.

Palazzi E, von Hardenberg J, Provenzale A (2013) Precipitation in the Hindu-Kush Karakoram Himalaya:observations and future scenarios. J Geophys Res Atmos 118:85−100

Palazzi, E., von Hardenberg, J., Terzago, S., & Provenzale, A. (2015). Precipitation in the Karakoram-Himalaya: a CMIP5 view. *Climate Dynamics*, *45*(1-2), 21-45.

Parvaze S, Ahmad L, Parvaze S, Kanth R. H. 2017. Climate Change Projection in Kashmir Valley (J&K). Curr World Environ, 12(1). pp 107-115. DOI:http://dx.doi.org/10.12944/CWE.12.1.13

Perkins, S. E., A. J. Pitman, N. J. Holbrook, and J. McAneney. 2007. Evaluation of the AR4 climate models' simulated daily maximum temperature, minimum temperature, and precipitation over Australia using probability density functions. Journal of climate 20(17): 4356-4376.

Pervez MS, Henebry GM (2014) Projections of the Ganges–Brahmaputra precipitation—Downscaled from GCM predictors. J Hydrol 517: 120-134. doi:10.1016/j.jhydrol.2014.05.016

Rajbhandari, R., Shrestha, A. B., Nepal, S., & Wahid, S. (2016). Projection of future climate over the Koshi River basin based on CMIP5 GCMs. Atmospheric and Climate Sciences, 6(02), 190.

Sachindra DA, Huang F, Barton A, Perera BJC. 2014. Statistical downscaling of general circulation model outputs to precipitation-part 1: calibration and validation. International Journal of Climatology 34(11): 3264–3281. https://doi.org/10.1002/joc.3914.

Salvi K, Kannan S, Ghosh S. 2013. High-resolution multisite daily rainfall projections in India with statistical downscaling for climate change impacts assessment. Journal of Geophysical Research: Atmospheres 118(9): 3557–3578. https://doi.org/10.1002/jgrd.50280

Salvi, K., & Ghosh, S. (2013). High-resolution multisite daily rainfall projections in India with statistical downscaling for climate change impacts assessment. Journal of Geophysical Research: Atmospheres, 118(9), 3557-3578.

Salvi, K., Kannan, S., & Ghosh, S. (2011). Statistical downscaling and bias-correction for projections of Indian rainfall and temperature in climate change studies. In 4th International Conference on Environmental and Computer Science (pp. 16-18).

Sanjay, J., Krishnan, R., Shrestha, A. B., Rajbhandari, R., & Ren, G. Y. (2017). Downscaled climate change projections for the Hindu Kush Himalayan region using CORDEX South Asia regional climate models. Advances in Climate Change Research, 8(3), 185-198.

Sati, S. P., & Gahalaut, V. K. (2013). The fury of the floods in the north-west Himalayan region: the Kedarnath tragedy. Geomatics, Natural Hazards and Risk, 4(3), 193-201.

Semenov MA, Barrow EM. 2002. LARS-WG, A Stochastic Weather Generator for Use in Climate Impact Studies, User Manual.

Semenov, M. 2008. Simulation of extreme weather events by a stochastic weather generator. Clim. Res. 35, 203–212.

Sharma, C., Arora, H., & Ojha, C. S. P. 2015 Assessment of the Effect of Climate Change on Historical and Future Rainfall in Uttarakhand.20th International Conference on

Hydraulics, Water Resources and River Engineering. IIT Roorkee, India, 17-19 December, 2015. DOI: 10.13140/RG.2.1.4356.3286

Shashikanth, K., & Sukumar, P. (2017). Indian Monsoon Rainfall Projections for Future Using GCM Model Outputs Under Climate Change. Advances in Computational Sciences and Technology, 10(5), 1501-1516.

Shashikanth, K., Madhusoodhanan, C. G., Ghosh, S., Eldho, T. I., Rajendran, K., & Murtugudde, R. (2014). Comparing statistically downscaled simulations of Indian monsoon at different spatial resolutions. Journal of hydrology, 519, 3163-3177.

Shrestha, A.B., Devkota, L.P., 2010. Climate Change in the Eastern Himalayas: Observed Trends and Model Directions. Climate Change Impact and Vulnerability in the Eastern Himalayas. ICIMOD, Kathmandu. Technical Report 1.

Singh, D., Jain, S. K., & Gupta, R. D. (2015). Statistical downscaling and projection of future temperature and precipitation change in middle catchment of Sutlej River Basin, India. Journal of Earth System Science, 124(4), 843-860.

Srinivas, V. V., Basu, B., Nagesh Kumar, D., & Jain, S. K. (2014). Multi-site downscaling of maximum and minimum daily temperature using support vector machine. International Journal of Climatology, 34(5), 1538-1560.

Thomas, L., Dash, S. K., Mohanty, U. C., & Babu, C. A. (2018). Features of western disturbances simulated over north I ndia using different land-use data sets. Meteorological Applications, 25(2), 246-253.

Timbal, B., P. Hope, and S. Charles, 2008: Evaluating the consistency between statistically downscaled and global dynamical model climate change projections. J. Climate, 21, 6052–6059.

Tripathi, S., Srinivas, V. V., & Nanjundiah, R. S. (2006). Downscaling of precipitation for climate change scenarios: a support vector machine approach. Journal of hydrology, 330(3-4), 621-640.

Wilby RL, Dawson CW, Barrow EM. 2002b. SDSM – a decision support tool for the assessment of regional climate change impacts. Environmental Modelling & Software 17: 145–157.

Wilby, R. L., Hay, L. E., & Leavesley, G. H. (1999). A comparison of downscaled and raw GCM output: implications for climate change scenarios in the San Juan River basin, Colorado. Journal of Hydrology, 225(1-2), 67-91.

Wilby, R., and T. Wigley, 1997: Downscaling general circulation model output: A review of methods and limitations. Prog. Phys. Geogr., 21, 530548.

Wilks DS. 1995. Statistical Methods in the Atmospheric Sciences. Academic Press: Orlando, FL.

Wiltshire, A.J., 2014. Climate change implications for the glaciers of the Hindu Kush, Karakoram and Himalayan region. Cryosphere 8, 941e958. http://dx.doi.org/10.5194/tc-8-941-2014.

Wu, J., Xu, Y., & Gao, X. J. (2017). Projected changes in mean and extreme climates over Hindu Kush Himalayan region by 21 CMIP5 models. *Advances in Climate Change Research*, *8*(3), 176-184.

Zambrano-Bigiarini M 2014 hydroGOF: Goodness-of-fit functions for comparison of simulated and observed hydrological time series; R package version 0.3-8.

Zorita E, von Storch H. 1999. The analog method as a simple statistical downscaling technique: Comparison with more complicated methods. Journal of Climate 12: 2474–2489

Figures

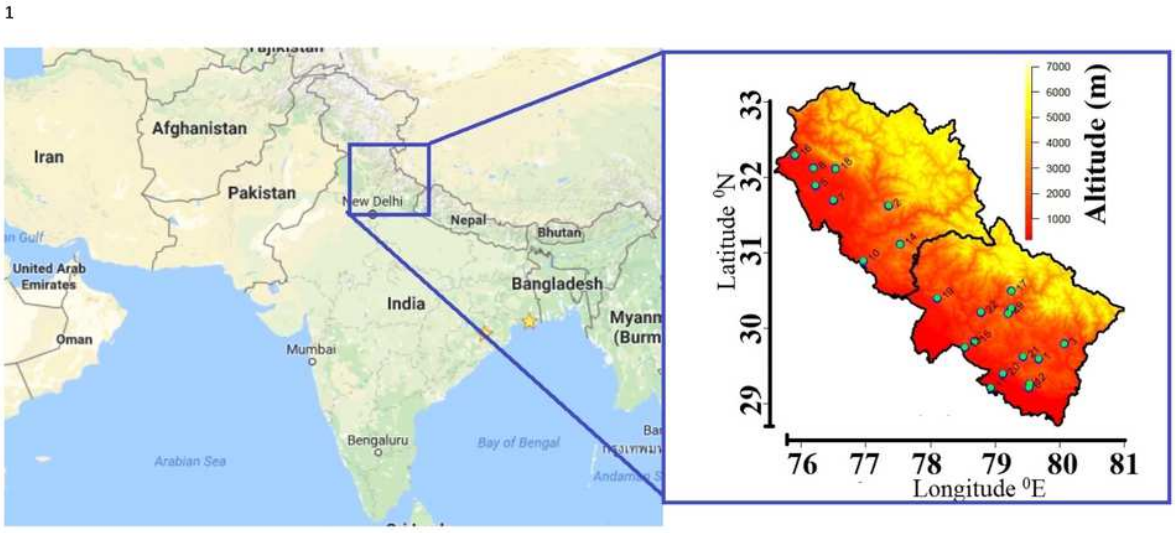

Figure 1

(left) The location of the study region by highlighted box over the map of India. (right) The distribution of 22 numbers of meteorological stations over the study region.

2

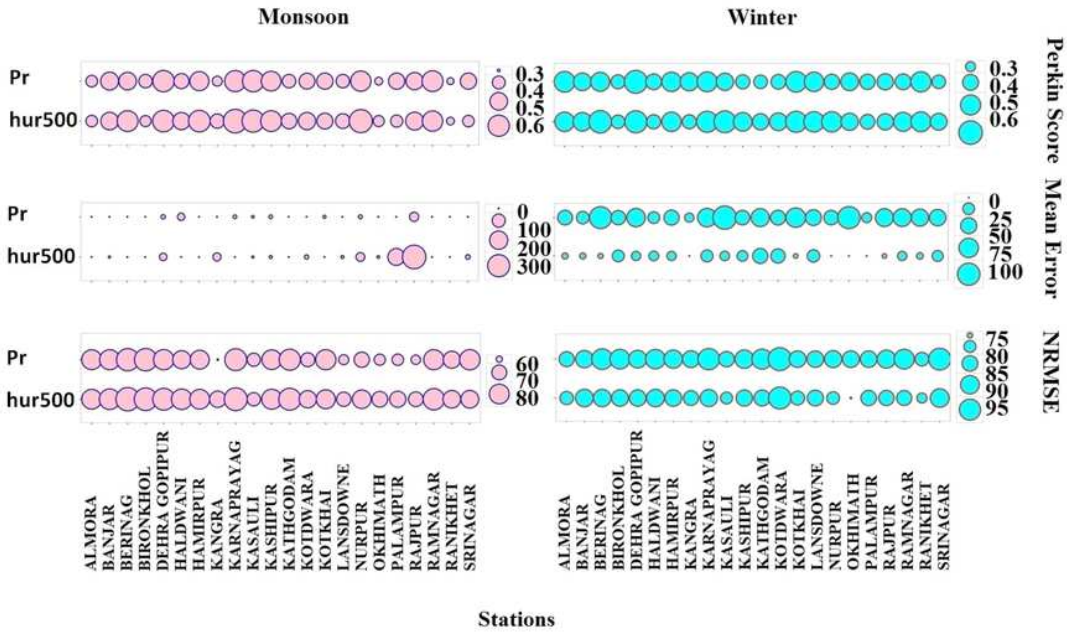

Figure 2

Performance of selected predictors for all the rain gauge stations using different skill scores viz. Perkin score, Mean error and NRMSE during the time window of 1951-1980 (calibration period) in the monsoon and winter season. Skill scores represents the ensemble mean skill scores of all the GCMs.

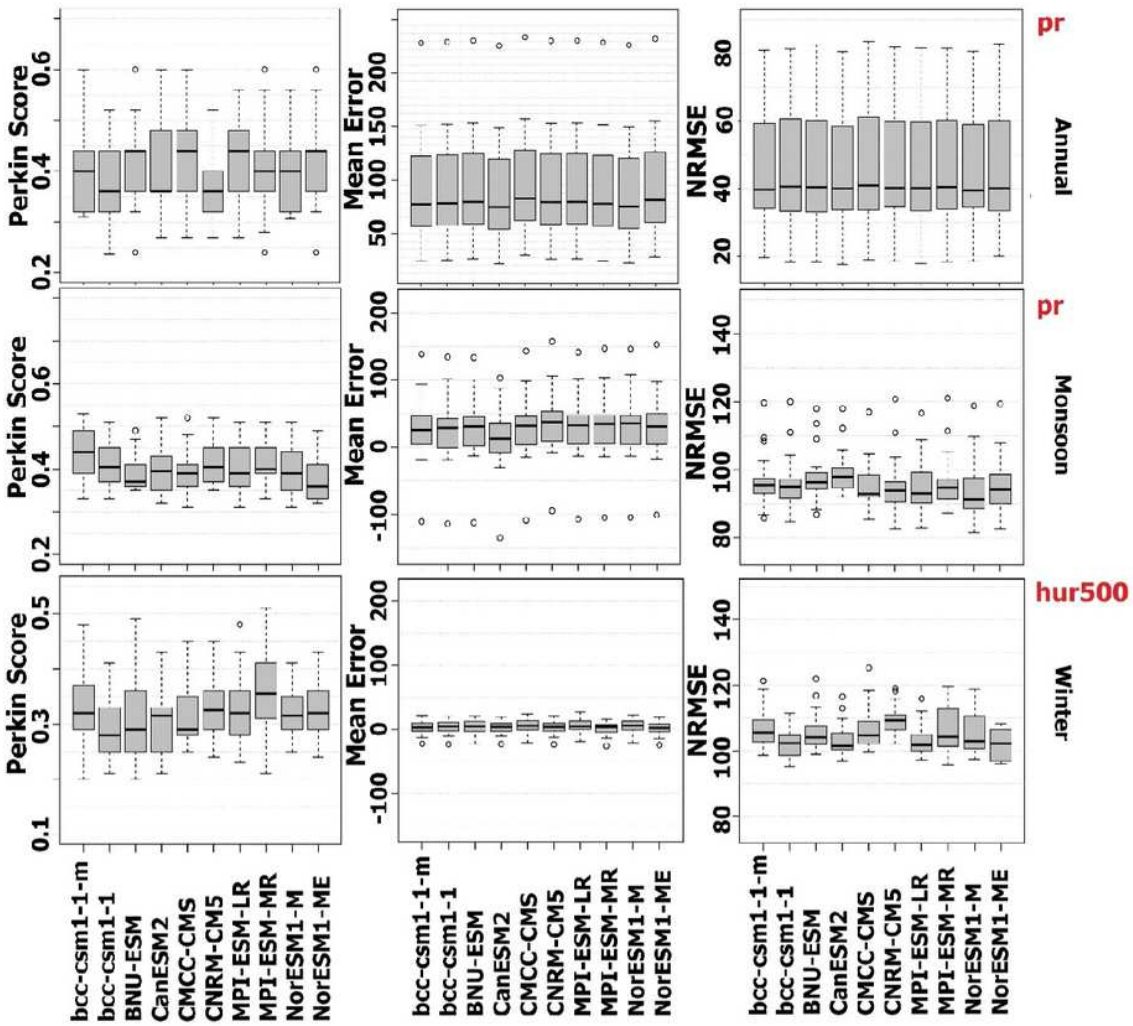

Figure 3

Performance of selected predictors for different GCMs using different skill scores viz. Perkin score, Mean error and NRMSE during the time window of 1981-2005 (validation period) in the annual, monsoon season and winter season. Here the box plot for a particular GCM was generated using the calculated values of skill scores of all the stations. For example, the box plot for BNU-ESM Perkin score in the winter season was calculated using the twenty two Perkin score values of 22 number of stations downscaled using BNU-ESM GCM in the winter season.

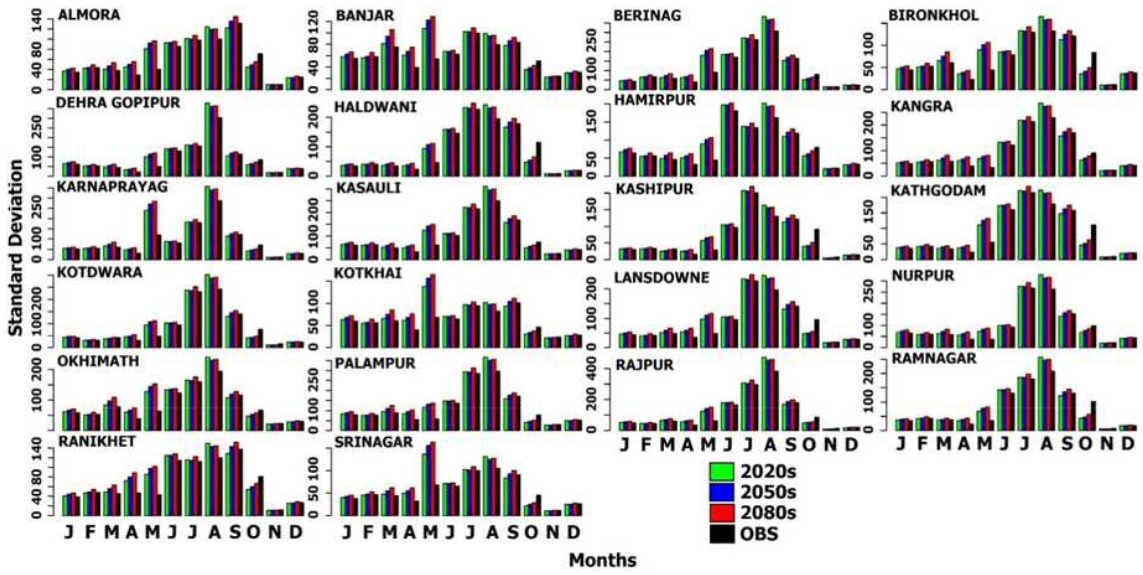

Figure 4

Downscaled standard deviation of monthly precipitation (using the predictor 'pr') in all the stations locations during different sub-periods in future. Standard deviation values of the multi model ensemble were represented through green colour bars (first) for 2020s, blue colour bars (second) for 2050s and red colour bars (third) for 2080s. The observed standard deviation during the period 1951-2005 were represented through the black colour bar (fourth).

6

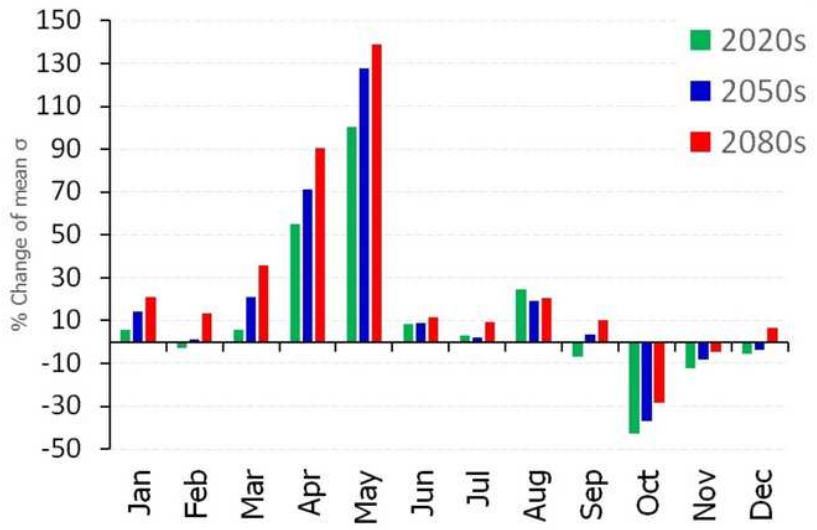

Figure 5

Month wise percentage change of standard deviation (σ, average standard deviation values of all the stations) of downscaled precipitation during different sub-periods. The results were shown for the downscaled precipitation using the 'pr' predictor.

Supplementary Files

This is a list of supplementary files associated with this preprint. Click to download.

- TableMeherDasTAAC14022022.pdf